Use of chènevotte, a valuable co-product of industrial hemp fiber, as adsorbent for copper ions: Kinetic studies and modeling

Chiara Mongioví, Dario Lacalamita, Nadia Morin-Crini, Xavier Gabrion, Vincent Placet, Ana Rita Lado Ribeiro, Aleksandra Ivanovska, Mirjana Kostić, Corina Bradu, Jean-Noel Staelens, et al.

Arabian Journal of Chemistry (2022) **15**, 103742

King Saud University

Arabian Journal of Chemistry

www.ksu.edu.sa
www.sciencedirect.com

ORIGINAL ARTICLE

Use of chènevotte, a valuable co-product of industrial hemp fiber, as adsorbent for copper ions: Kinetic studies and modeling

Chiara Mongioví [a], Dario Lacalamita [a], Nadia Morin-Crini [a], Xavier Gabrion [b], Vincent Placet [b], Ana Rita Lado Ribeiro [c], Aleksandra Ivanovska [d], Mirjana Kostić [e], Corina Bradu [f], Jean-Noël Staelens [g], Bernard Martel [g], Marina Raschetti [b], Grégorio Crini [a,*]

[a] *Laboratoire Chrono-environnement, UMR 6249, UFR Sciences et Techniques, Université Bourgogne Franche-Comté, 16 route de Gray, 25000 Besançon, France*
[b] *FEMTO-ST, Department of Applied Mechanics, Université Bourgogne Franche-Comté, 16 route de Gray, 25000 Besançon, France*
[c] *Laboratory of Separation and Reaction Engineering – Laboratory of Catalysis and Materials (LSRE-LCM), Faculdade de Engenharia, Universidade do Porto, Rua Dr. Roberto Frias s/n, 4200-465 Porto, Portugal*
[d] *Department of Textile Engineering, Innovation Center of the Faculty of Technology and Metallurgy, University of Belgrade, Karnegijeva 4, 11000 Belgrade, Serbia*
[e] *Department of Textile Engineering, Faculty of Technology and Metallurgy, University of Belgrade, Karnegijeva 4, 11000 Belgrade, Serbia*
[f] *University of Bucharest, Department of Systems Ecology and Sustainability, PROTMED Research Centre, Spl. Independentei 91-95, 050095 Bucharest, Romania*
[g] *Univ. Lille, CNRS, INRAE, ENSCL UMR 8207, UMET – Unité Matériaux et Transformations, Lille, France*

Received 25 November 2021; accepted 24 January 2022
Available online 29 January 2022

KEYWORDS

Hemp shives;
Adsorbent;
Copper;
Batch;
Kinetics;
Modeling

Abstract In this study, a series of hemp shives (chènevotte) with different chemical compositions and properties, namely a raw (SHI-R), a washed with water (SHI-W), three samples chemically modified with KOH (SHI-OH), Na_2CO_3 (SHI-C) or H_3PO_4 (SHI-H), and a hemp shives sample prepared by grafting of carboxylic groups (SHI-BTCA), were used as adsorbents for the removal of copper present in aqueous solutions. This article presents the abatements and kinetics obtained using batch experiments and their modeling. The results first showed that the quantity of copper removed depended on the used shives and the copper initial concentration. At the same experimen-

* Corresponding author.
E-mail address: gregorio.crini@univ-fcomte.fr (G. Crini).
Peer review under responsibility of King Saud University.

Production and hosting by Elsevier

https://doi.org/10.1016/j.arabjc.2022.103742

tal conditions, SHI-C and SHI-BTCA samples possessed similar performances which are significantly higher than those of other studied hemp shives. Copper adsorption reached equilibrium after 60 min of contact time and was independent of concentration in the range 5–150 mg/L for SHI-C and SHI-BTCA. According to the better Chi-squared values, the experimental data were better simulated by the non-linear kinetic model in the order: Lagergren < Elovich < Ho and McKay < -Weber and Morris < Boyd for SHI-C and Boyd < Ho and McKay < Weber and Morris < Lagergren < Elovich for SHI-BTCA. The analysis of data indicated that chemisorption is the main mechanism for binding copper onto SHI-BTCA, while physisorption (diffusion) is the main interaction for copper adsorption onto SHI-C. The adsorption-oriented process using hemp shives could be an advantageous approach for recovering copper from metal industry effluents due to the simplicity of the process, its efficiency to treat both diluted and concentrated copper solutions, and the low-cost, non-toxic to humans and the environment, ecological character, and facile use of hemp shives.

1. Introduction

Plants have been largely forgotten by modern technology. Increasingly, however, the bio-economy approach has been targeted as a key element for smart, green growth, with a return to the forefront of annual plants such as hemp, flax and jute. Indeed, the evolution of production and transformation processes (food sector, bioenergy), the need for materials compatible with sustainable construction, consumer expectations for quality products and regulatory requirements are driving manufacturers to turn to resources of biological origin (called biomass), which are renewable and have little or even no impact on the environment.

Among the different sources of biomass available for further processing, the hemp plant (*Cannabis sativa* L.), referring to industrial hemp, is an environmentally and agriculturally beneficial crop (Crini and Lichtfouse, 2020). Hemp differs stands out in comparison to other crops as it is inexpensive, ecological and sustainable, requires neither pesticides nor high volumes of water to grow; it contributes to soil improvement, is carbon neutral, and has low embodied energy consumption. It is also very interesting to note that the whole plant is recoverable for a wide variety of applications. As a multi-use plant, hemp has traditionally been a source of a variety of products, such as cordages, apparel, fabrics, building materials and papers from fibers or flour and oil from seeds. Applications are also found in functional food, beverages, biocomposites (bioplastics, automotive composites), cosmetics, energy and fuel production, jewelry and fashion sectors. In Europe, hemp production is currently undergoing a renaissance, with France being the largest hemp producer (Kostić et al., 2014; Dunford, 2015; Ingrao et al., 2015; Crini et al., 2020).

The hemp plant is cultivated for its fibers from the stalk and its oil from the seeds. The hemp industry also produces by-products called chènevotte, shives or hurds, which form the inner woody core of the stalks. These by-products, for long considered as wastes, found novel applications in the fields of paper, construction and composites (known as hemp concrete). Traditionally, hemp shives were used for soil improvement, animal bedding or to prepare particleboards for building insulation (Crini and Lichtfouse, 2020). Thanks to their absorbent properties (e.g., for the adsorption of odors and liquids), they are used in horse stalls. Hemp shives are also a lightweight material known for its insulating properties. Mixed with binders (lime and/or cement) and water, they produce hemp concrete (3D printed lightweight composite) for construction. They have also been studied as a resource for reinforcements in bioplastics (injection molded polypropylene biocomposites). The chemical composition of hemp shives is characterized by a high content of polysaccharides such as cellulose and hemicelluloses, valuable biopolymers in green chemistry. For example, these biopolymers can yield different thermochemical conversion products (biorefinery concept), e.g., the production of sugar-rich bio-oil, energy, biofuel or biodiesel, which are part of the bio-economy concept. However, to our knowledge, there are not yet any real applications of hemp shives as adsorbents of environmental pollutants (Crini and Lichtfouse, 2020; Crini et al., 2020).

For the past year, as part of a trans-disciplinary European research project (FINEAU project 2021-2024) involving French, Serbian, Italian, Portuguese and Romanian university groups, a French agricultural cooperative and two surface-treatment industries, we have been working on the use of chènevotte (hemp shives) for potential applications in the remediation field. The first objective of this project was to prepare materials based on hemp shives. This raw co-product of the hemp industry, noted SHI-R, was thus chemically modified using protocols implemented by one of the industrial partners of the project. The shives were either washed (sample SHI-W) or activated by chemical reagents such as KOH (SHI-OH), Na_2CO_3 (SHI-C) and H_3PO_4 (SHI-H). Another material was obtained from grafting of carboxylic groups (SHI-BTCA sample) through the use of 1,2,3,4-butanetetracarboxylic acid (BTCA). In a recent paper (Mongioví et al., 2021), we prepared and characterized modified hemp shives using spectroscopic and microscopic techniques in order to obtain information on the structure and morphology of the samples. The second objective of the FINEAU project is to use these materials to recover and valorize the copper present in industrial effluents.

Copper has become ubiquitous in our lives: household appliances, high-tech products, electrical installations, telecommunications, motors, energy, wind turbines and solar systems, architecture, agriculture, viticulture, biomedical applications, food supplements, and paint industry (Barakat and Kumar, 2015; Qasem et al., 2021). Due to its extensive use in many areas, copper is found in all compartments of the environment. Copper, like some other metals, contaminates water and soil, disturbs ecosystems, and accumulates in the food chain. The presence of copper in aqueous compartments has been the subject of numerous studies over the last 20 years, both in terms of its fate and behavior, as well as its toxicity (Solioz, 2018). Metal industries in general and particularly the surface treatment industry, are one of the sources of copper emissions into the environment. Copper is typically present at concentrations of about a few hundred micrograms to a few milligrams per liter in the discharged water of the surface treatment industries (its authorized limit value is 2 mg/L). This metal is considered as a priority substance by the French Water Agency with the aim of reducing its presence or suppressing it completely. Copper, together with other seven toxic metals, is also used in the calculation of an indicator known as the metox index, which is used to quantify certain toxic forms of pollutions and to calculate the taxes that industrials must then pay to the Water Authority. Thus, one of the objectives of the industrialists is to decrease the copper content in the discharges. However, this challenge is difficult because conventional methods to treat trace amounts of copper are expensive for small

industrial structures. Therefore, innovation is needed to find elimination methods that are technologically simple, chemically effective, and economically viable (Al-Saydeh et al., 2017; Torres, 2020; Elgarahy et al., 2021; Paliulis, 2021; Rashid et al., 2021). Many studies are also focusing on the recovery and reclamation of copper from low concentration effluents (Zare et al., 2015; Wahid et al., 2017; Lopičić et al., 2019; Lessa et al., 2020; Jamoussi et al., 2020). This aspect is pertinent because the price of copper is constantly increasing due to growing demand. Indeed, with the development of green technologies, especially in the field of energy and electric vehicles, the demand for copper is constantly increasing. Moreover, copper has the remarkable property of being infinitely recyclable and reusable without loss of performance or properties. Thus, the aspect of recycling used copper is of interest not only for the industrial sector but also for the academic community. Finding simple, efficient, cheap and environmentally friendly recovery methods is, therefore, an interesting challenge.

In this study, we evaluated the adsorption properties of raw and modified hemp shives to recover copper from aqueous solutions. Here, studies concerning the effect of copper concentration, adsorbent dose and contact time were evaluated using the batch method. In order to model experimental data, the adsorption and diffusion kinetic constants were determined using the common empirical equations of Lagergren, Ho and McKay, Weber and Morris, Elovich, and Boyd.

2. Material and methods

2.1. Hemp shives and reagents

Chènevotte or raw shives (SHI-R, Fig. 1) as co-product of the hemp industry were provided by Eurochanvre (Arc-les-Gray, France). These commercial shives (0.90 euros/kg) are constituted of parallelepiped particles varying in length (from 5 up to 25 mm) and are intended for plant and animal mulching, and insulation. Copper(II) sulfate was purchased from Sigma-Aldrich (France) and used as received. Appropriate weight of this salt was dissolved in water to obtain a stock solution containing 300 mgCu/L (initial pH of the metal solution 4.5 ± 0.1). Solutions with lower copper concentrations (1–200 mg/L; initial pH in the range 4.9–5.5) were obtained by diluting the stock solution. The copper concentration in all solutions was determined by inductively coupled plasma atomic emission spectroscopy (ICP-AES) following a standard protocol prior to each experiment. All other reagents (p.a. purity) obtained from commercial sources were used as received.

2.2. Modification of the hemp shives

Raw shives (SHI-R) were modified by acidic or alkaline activation or by grafting. The procedures performed to modify the raw shives by activation were recently detailed (Mongioví et al., 2021). Briefly, SHI-R samples were first washed several times with osmosed water under agitation at room temperature until the wash water became clear. The shives were then separated by filtration and dried under vacuum at 80 °C for one day (the obtained shives are noted SHI-W).

The dry SHI-W samples were activated using acidic or alkaline solutions as follows: 1 L of 30% H_3PO_4, KOH (1 M) or Na_2CO_3 (1 M) solution was slowly poured on 30 g of shives placed in a beaker. Then, the solution was heated at 40 °C and the treatment lasts 4 h. After cooling, the solution was stirred with a vortex mixer for 1 h at room temperature and abandoned for 12 h. The mixture was filtered and the recovered shives were extensively washed with osmosed water (until neutral pH), and dried under vacuum at 80 °C for one day. Such treated shives with H_3PO_4, KOH or Na_2CO_3 are marked as SHI-H, SHI-OH, or SHI-C, respectively.

Fig. 1 Chènevotte or raw hemp shives (SHI-R).

A grafting reaction using 1,2,3,4-butanetetracarboxylic acid (BTCA) as cross-linking agent was used in order to introduce specific chelating groups onto shives surface according to the already published synthesis (Loiacono et al., 2017). Briefly, SHI-W were pre-treated with 1 M NaOH for 3 days at ambient temperature under mechanical stirring and then filtered, washed with distilled water until neutral pH, and dried at 60 °C for 15 h. Samples were then immersed in an aqueous solution containing 100 g/L of BTCA and 30 g/L of NaH_2PO_2 for 15 h at ambient temperature under mechanical stirring. After draining, shives were spread on the bottom of a glass crystallizer and put in a ventilated oven at 160 °C for 90 min. They were suspended in distilled water overnight under stirring, filtered, thoroughly washed with distilled water, and dried in a ventilated oven at 60 °C for 15 h. The shives were finally activated by converting the carboxylic groups into carboxylate groups by their immersion in a sodium bicarbonate solution (20 g/L) under mechanical stirring for 24 h. The obtained material was denoted as SHI-BTCA.

2.3. Characterization of the samples

The chemical composition of the samples was determined according to procedure recently published by Mongioví et al. (2021) and given in Table 1.

The ion exchange capacity (IEC) of each sample was determined by a pH-metric titration according to the calcium acetate method (Ducoroy et al., 2007).

Table 1 Characteristics of the hemp shives samples.

Sample	SHI-R	SHI-W	SHI-H	SHI-OH	SHI-C	SHI-BTCA
α-cellulose (%)	55.53	56.93	61.67	62.30	62.93	36.58
Hemicelluloses (%)	12.48	15.42	9.26	5.08	9.58	12.57
Klason lignin (%)	26.54	26.70	25.78	31.62	26.59	39.60
Pectins (%)	0.43	0.79	0.92	0.33	0.42	3.21
Fats and waxes (%)	0.72	0.38	0.09	0	0.04	0.76
IEC[a] (meq/g)	0.10	0.13	0.63	0.14	0.31	1.50
Volume of the pores[b] (μm^3)	72.9	75.3	74.4	72.0	68.9	49.5

[a] Ion-exchange capacity.
[b] From nanotomography measurements (diameter greater than 1 μm).

Elemental analysis of the hemp shives surfaces was performed using the Thermo Noran system for energy-dispersive X-ray spectroscopy (EDS) and electron beam excitation with a voltage from 15 keV to 20 keV.

The computed nano-tomography (nano-CT) investigation was performed with an RX Solution EasyTom 160 equipped with an X-ray source Hamamatsu Open Type Microfocus L10711 (EasyTom, Chavanod, France). The X-ray transmission images were acquired using a detector 2530DX of 2176×1792 pixels^2. The tube voltage and the tube current used were 60 keV and 86 μA, respectively. The exposure time was set at 6 images/s with an average frame of 6 images. A total of 1440 projections were collected for each sample resulting in a time of 30 min per tomograph. The entire volume was reconstructed at a full resolution with a voxel size of 1.4 μm corresponding to a field of view of 2.8×2.5 mm^2, using filtered back-projection. The data analysis for porosity measurement was then processed using VG StudioMax software (Version 3.5, Heidelberg, Germany). The segmentation was realized using visually interpreted thresholds and prior knowledge. Indeed, the grey level depends on the density of the material. Two distinct peaks were found in the multimodal image histogram. These peaks were attributed to air, and cell wall material, respectively. Thresholds were then positioned between the respective peaks and each material was then represented by a color: air in grey, cell walls in white. The porosity measurements were performed on 2 representative cubes of 0.125 μm^3 artificially taken after each segmentation. The volume of pores (V_p, in μm^3) is calculated using Eq. (1), where V_c is the volume of the cube and V_m is the volume of material (Jiang et al., 2017). The values of porosity are reported in Table 1.

$$V_p = V_c - V_m \tag{1}$$

2.4. Copper ion adsorption experiments

Adsorption kinetics were determined by the batch technique using the following protocol. In each experiment, 100 mL of a copper solution of known concentration were added to 0.5–3 g of hemp shives in a 250 mL round bottom flask at 22 ± 1 °C. The initial pH of each metal solution was in the range 4.5–5.5 depending on the initial metal concentration. The mixture was then mechanically stirred for a given time on a rotating shaker at a constant speed (250 rpm). After treatment, the shives were removed by filtration. The final metal concentration in the solution was then determined and the adsorption capacity, i.e., the amount of metal adsorbed per gram of adsorbent, was calculated. Initial copper concentration (range 1–300 mg/L), adsorbent dose (0.5, 1, 2 and 3 g), and contact time (range 1–120 min) were varied to investigate their effect on the hemp shives adsorption capacity. All experiments were replicated (n = 3–5) under identical conditions.

The amount of copper adsorbed at time t by one gram of materials (q_t, mg/g) was calculated from the mass balance Eq. (2), where C_o and C_t are the initial and final copper concentrations in the solution (mg/L), respectively, V is the volume of sorbate solution (L) and m is the mass of adsorbent used (g). Eq. (2) can be rewritten as Eq. (3), where q_e (mg/g) and C_e (mg/L) are the amount of copper adsorbed at equilibrium and the equilibrium copper concentration in the solution, respectively. In this study, the copper removal (R in %) was also calculated by using Eq. (4).

$$q_t = \frac{V(C_o - C_t)}{m} \tag{2}$$

$$q_e = \frac{V(C_o - C_e)}{m} \tag{3}$$

$$R = \frac{100(C_o - C_t)}{C_o} \tag{4}$$

2.5. Kinetic models

To describe the experimental kinetic data and to investigate the copper adsorption mechanism onto hemp shives, five commonly used but empirical kinetic models (Schwaab et al., 2017; Tran et al., 2017; Kajjumba et al., 2018; Benjelloun et al., 2021; Bullen et al., 2021), namely Lagergren (pseudo-first-order, Eq. (5); Lagergren, 1898), Ho and McKay (pseudo-second-order, Eq. (6); Ho and McKay, 1998a,b), Weber and Morris (intra-particle diffusion model, Eq. (7); Weber and Morris, 1963), Elovich (Eq. (8); Elovich and Larinov, 1962), and Boyd (Eqs. (9) and (10); Boyd et al., 1947a,1947b) models were tested to find the best-fitting one. In the corresponding linear equations (Eqs. (5)–(10)), q_t and q_e (mg/g) are the copper amounts adsorbed at time t (min) and at equilibrium (mg/g), respectively; k_1, k_2, k_i, α and β are the pseudo-first order rate constant (1/min), equilibrium rate constant of pseudo-second order (g/mg min), intraparticle diffusion rate constant (mg/g min$^{1/2}$) and Elovich rate constants (g/mg min), respectively; in the Weber and Morris equation, C is the intercept (mg/g); in the Boyd model, F is the fractional attainment of

equilibrium at time t obtained by the ratio between the amounts adsorbed at time t and infinite time, S (mL/min) is the rate constant and Bt is a calculated mathematical function of F. To evaluate the validity of each kinetic model, the results obtained by the fitting of experimental data with each kinetic model were analyzed using the linear regression coefficients of determination (R^2) and the Chi-square test (χ^2). The lowest χ^2 value indicates that the applied kinetic models is more appropriate than others.

$$log(q_e - q_t) = logq_e - \frac{k_1}{2.303}t \quad (5)$$

$$\frac{t}{q_t} = \frac{1}{k_2 q_e^2} + \frac{1}{q_e}t \quad (6)$$

$$q_t = k_i t^{1/2} + C \quad (7)$$

$$q_t = \frac{\ln(\alpha\beta)}{\beta} + \frac{1}{\beta}\ln t \quad (8)$$

$$ln(1 - F) = -St \quad (9)$$

$$Bt = -0.4977 - \ln(1 - F) \quad (10)$$

3. Results and discussion

3.1. Hemp shives characteristics

The results reported in Table 1 shows that significant changes in the chemical composition of each sample after treatment as well as in surface morphology and roughness were observed, which were recently discussed elsewhere by Mongioví et al. (2021). Briefly, an increase in the percentage of cellulose and a decrease of hemicelluloses content was observed for all the samples after activation treatment, except for SHI-BTCA that showed a completely different chemical composition due the grafting reaction. Alkaline (SHI-C and SHI-OH samples) and acid (SHI-H) treatments resulted in the reduction of hemicelluloses content. The volume of the pores, obtained from nano-tomography measurements, was comparable for all the raw, washed and activated samples, while for the grafted sample (SHI-BTCA) a significant decrease was observed. Moreover, for this later material, the grafting with BTCA led to an important increase in the IEC values (Table 1).

3.2. Effect of hemp shives modifications on copper removal

The comparison between unmodified (SHI-R and SHI-W) and chemically modified (SHI-OH, SHI-C, SHI-H and SHI-BTCA) hemp shives adsorption capacities for copper (initial concentration of 150 mg/L), is presented in Fig. 2. With exception of hemp shives modified with acid (SHI-H), all other modified shives showed improved ability to adsorb copper compared to the raw shives. The percentage of removed copper was in the order: SHI-C $\sim$ SHI-BTCA $>$ SHI-OH $\gg$ SHI-W $>$ SHI-R $\gg$ SHI-H. Indeed, hemp shives treated with sodium carbonate (SHI-C) or BTCA (SHI-BTCA) possessed the highest ($>$95%) adsorption capacities towards copper. In particularly, these two samples were able to remove 7 mg Cu per g adsorbent, whereas SHI-H, SHI-R, SHI-W and SHI-OH only removed 0.6, 2.85, 3.15 and 5.85 mg Cu/g adsorbent, respectively.

Higher adsorption performance of SHI-BTCA sample could be explained by the chemisorption (complexation, microprecipitation) and ion-exchange occurring due to the presence of numerous carboxylate groups (see the IEC value reported in Table 1). Indeed, the presence of these groups in sodium form allows both electrostatic attractions with metal ions and ion-exchange phenomena on the shives surface. This was verified by monitoring the copper and sodium concentrations in the supernatants after adsorption. When the initial copper concentration decreased due to adsorption, the sodium concentration increased, which was also reported by Loiacono et al. (2018b). The chemisorption mechanism is also sustained by another observation. At the end of each experiment, a slight pH variation between 0.5 and 0.8 units for SHI-C and SHI-OH samples, and between 0.8 and 1.5 units for SHI-BTCA were registered. Indeed, for SHI-BTCA, the initial pH of 5.0 $\pm$ 0.1 increased to a maximum value of 6.5 $\pm$ 0.1. At this pH, metal cations can start to precipitate, which also suggests the presence of microprecipitation phenomenon during adsorption.

No variation in pH was observed for SHI-R and SHI-W samples, while the pH decreased by 1 unit after the adsorption of copper onto SHI-H sample. The SHI-C and SHI-OH removal capacities could be related to significant changes in their chemical compositions (Table 1) and surface morphology (i.e., roughness) (Mongioví et al., 2021). On the other hand, lower IEC values of SHI-C and SHI-OH suggested that their higher capacities could be ascribed to the physisorption. The IEC values of SHI-R and SHI-W samples were weak and their adsorption performances remained limited (R $\sim$ 40–45%), whereas the SHI-H sample had a significantly reduced copper adsorption capacity due to the degradation of the structure, which was reported in the previously published paper (Mongioví et al., 2021).

3.3. Effect of initial copper concentration

The initial copper concentration was varied from 5 up to 300 mg/L in order to assess its effect on the adsorption efficiency of raw and differently modified hemp shives. The results presented in Fig. 3 showed that adsorption capacities of hemp shives followed the same order previously established (Fig. 2) independently of the initial concentration. However, for each sample, the quantity of the removed metal depended on the copper concentration in the aqueous solution. This is in agreement with those reported in similar studies(Mokkapati et al., 2016; Loiacono et al., 2018a,2018b; Rozumová and Legátová, 2018; Rozumová et al., 2018; Morin-Crini et al., 2019; Bashir et al., 2020; Tofan et al., 2020; Wong et al., 2020). As expected, when the copper concentration increased from 25 up to 300 mg/L, the copper removal significantly decreased. Such behavior is due to the increase in the number of metal ions competing for the available binding sites in the adsorbent and the lack of sites capable of binding Cu(II) ions at higher concentration levels.

It is noteworthy that among all samples, SHI-C and SHI-BTCA demonstrated high performances even at high copper concentrations. Until an initial metal concentration of 100 mg/L, the copper removal is almost 100% and decreased

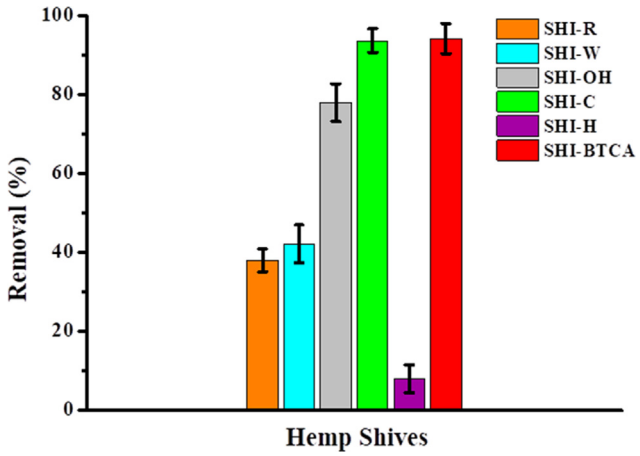

Fig. 2 Comparison between adsorption capacities of hemp shives expressed in % of removed copper (conditions: initial copper concentration 150 mg/L; pH 5; temperature 22 ± 1 °C; adsorbent dose 2 g/100 mL; contact time 120 min; n = 5).

to around 67% for an initial concentration of 300 mg/L (Fig. 3). However, when the initial copper concentration was between 5 and 100 mg/L, the copper removal was almost 100%, demonstrating that these samples are effective at both high and trace concentrations of copper. The above stated is interesting because the proposed SHI-C and SHI-BTCA shives could reduce the emission limit value for the copper present in the discharges of the French surface treatment industry, which is 2 mg/L. Furthermore, abatement values (R ~ 60–55%) obtained for the SHI-R sample at lower initial copper concentrations (range 5–50 mg/L) suggest that other interactions such as physical adsorption (diffusion) in the macromolecular network are also involved in the adsorption mechanism. This hypothesis can be related to the results concerning the SHI-H sample modified with H_3PO_4 acid. Such modified shives always possessed the lowest adsorption capacity, however, at

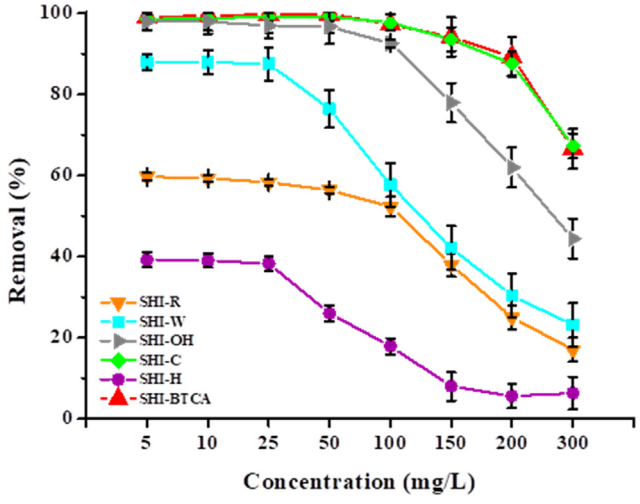

Fig. 3 Effect of the initial concentration on the removal (%) of copper by hemp shives (conditions: adsorbent dose 2 g/100 mL; contact time 120 min; temperature 22 ± 1 °C; n = 3).

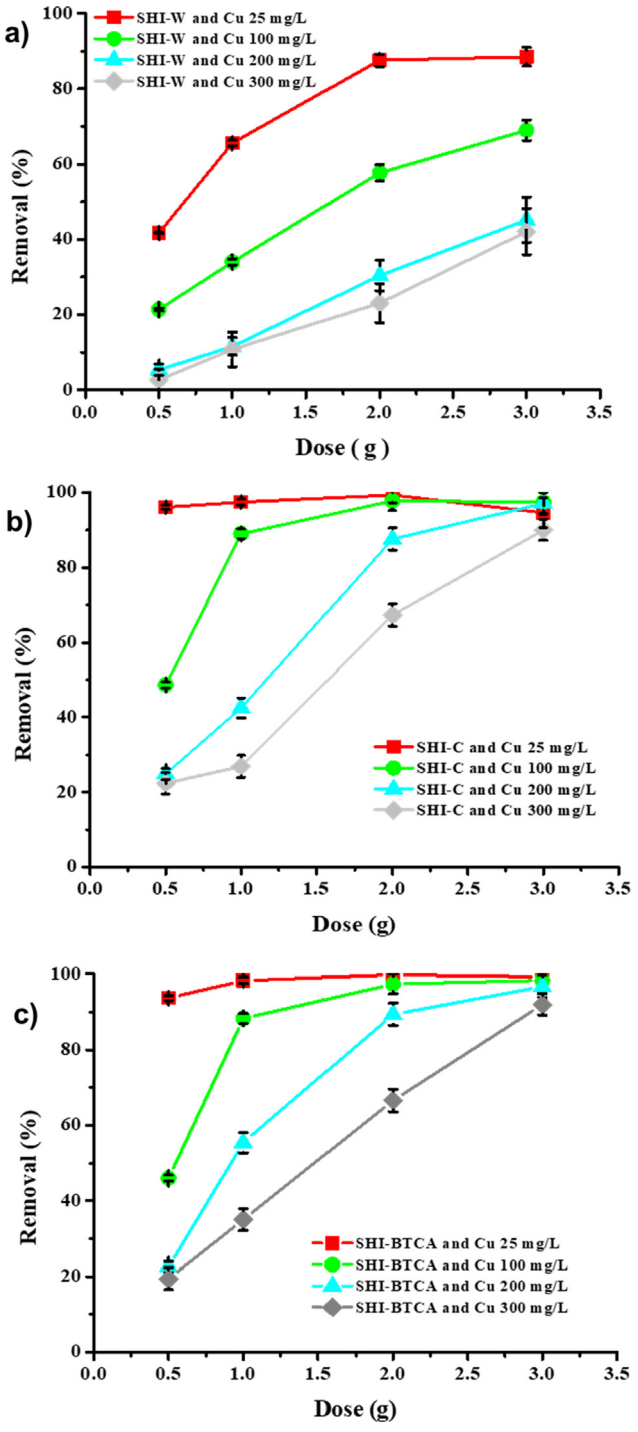

Fig. 4 Comparison of the copper removal (%) in presence of increasing doses of adsorbents (SHI-W (a), SHI-C (b), SHI-BTCA (c)) using a different initial metal concentrations (other conditions: volume of solution 100 mL; contact time 120 min; agitation speed 250 rpm; temperature 22 ± 1 °C; n = 3).

lower initial copper concentrations (between 5 and 25 mg/L), the copper removal is around 40%. Based on all above discussed, in further experiments, we compared the results of the two best performing samples (SHI-C and SHI-BTCA) with the SHI-W sample (taken as reference).

3.4. Effect of adsorbent dose on copper removal

The adsorption of copper ions on unmodified (SHI-W) and modified (SHI-C and SHI-BTCA) shives was studied by changing the adsorbent dose from 0.5 up to 3 g immersed in 100 mL of copper solutions having four initial concentrations (25, 100, 200 and 300 mg/L) whilst keeping constant the contact time (120 min), the agitation speed (250 rpm), the temperature (22 ± 1 °C) and the pH (range between 4.5 and 5.2). According to the results given in Fig. 4, it is evident that the percentage of removed copper increased by enhancing the adsorbent dose which could be attributed to the larger adsorbed surface and availability of more adsorption sites. This phenomenon is the most prominent in the case of washed sample (SHI-W) and also for activated (SHI-C) and grafted (SHI-BTCA) samples, in particular at higher concentrations (Fig. 4). A similar interpretation of the adsorbent dose *vs.* metal removal has been reported in other studies of lignocellulosic materials (Vaghetti et al., 2009; Reddy et al., 2012; Gupta et al., 2015; Lopičić et al., 2017; Wong et al., 2020). Moreover, it is important to emphasize that at the lowest initial copper concentration (25 mg/L), 0.5 g of samples was sufficient to obtain the best metal removal in the case of SHI-C and SHI-BTCA. On the contrary, for the highest initial copper concentration (300 mg/L), 2 g of samples are needed to obtain removal of about 67%.

Replacing conventional adsorbents with another innovative adsorbent implies that the latter provides a gain in performance at the same or lower cost. In the case of the SHI-C sample, usage of higher amount of adsorbent is not a problem because, on the one hand, the raw material (hemp shives SHI-R) is an abundant and cheap co-product (0.90 euros/kg), while on the other hand, sodium carbonate modification is a process already used by the industrial partner involved in this study. Furthermore, one of the objectives of our investigation is to propose technology for the selective recovery of copper from industrial effluents. Once used, the adsorbent containing copper would be incinerated, so its dose does not represent the limiting factor. The modification of the SHI-BTCA sample involves a chemical grafting reaction, which will necessarily increase the cost of the process, and, therefore, in this case, the adsorbent dose is a limiting factor. At comparable performances, the SHI-C sample is therefore more interesting to use than the SHI-BTCA sample.

3.5. Effect of contact time on the adsorption of copper ions

It is well known that besides the initial ion concentration, the contact time required to remove, complex or recover a metal present in an aqueous solution represents another factor affection the adsorption process. The influence of contact time on the adsorbents capacities (q_t) for copper ions present in various initial concentrations (ranging from 1 to 150 mg/L) is presented in Fig. 5. It is clear that in the case of copper concentrations up to 75 mg/L, the adsorbents q_t values increased with through the time and after a certain time reached equilibrium. Independently on the used initial copper concentrations, higher adsorption capacities were obtained using SHI-C and SHI-BTCA than SHI-W. The data clearly indicated that the adsorption process was uniform with time and can be considered as rapid since the largest amount of copper ions was

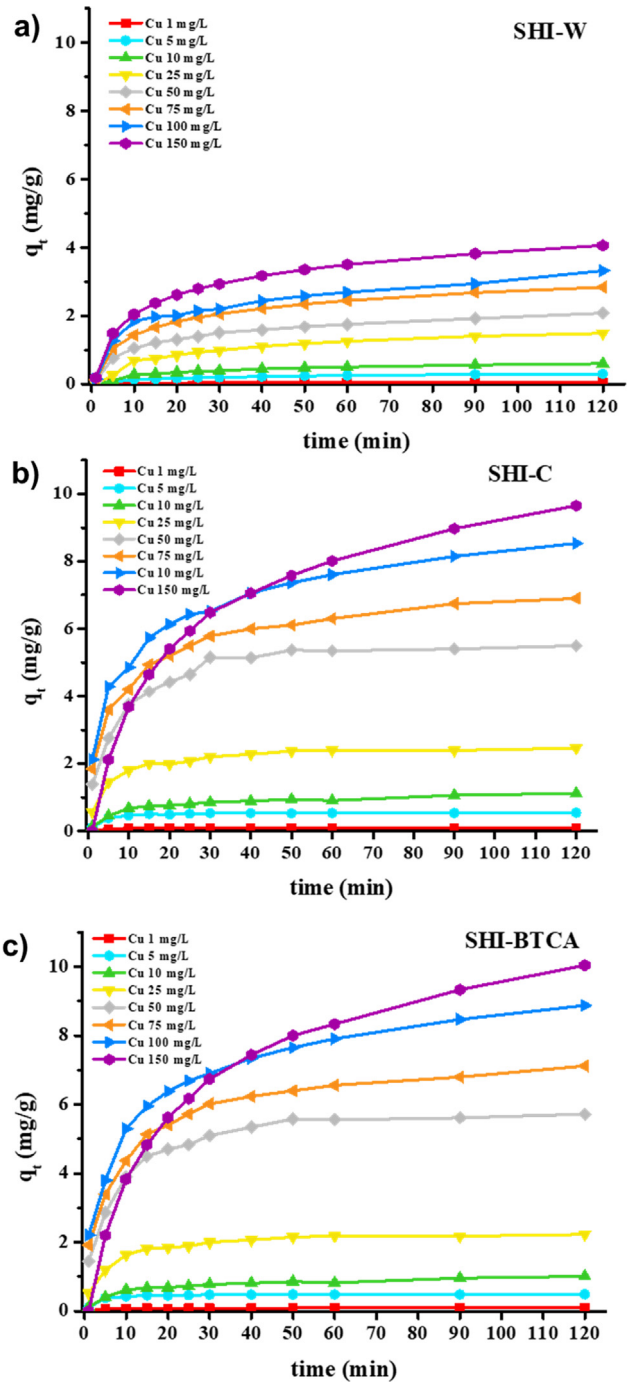

Fig. 5 Kinetics of adsorption of copper ions by hemp shives from an aqueous solutions containing different initial metal concentrations (other conditions: adsorbent dose 1 g; volume of solution 100 mL; agitation speed 250 rpm; temperature 22 ± 1 °C; n = 3).

adsorbed by the shives within the first 30 min of adsorption. After that, the values of q_t showed no significant difference by prolonging the contact time. In other words, at the beginning of the adsorption process, the presence of a large number of free sites for copper adsorption increased the q_t values. However, by extending the contact time, copper ions travel

within the adsorbent pores, the number of free sites decreased, thus reducing the copper adsorption reaching a plateau (Ivanovska et al., 2021). As expected, the overall trend was an increase of the adsorption capacity with increasing metal concentration, confirming strong interactions between copper and the two mentioned samples SHI-C and SHI-BTCA. The adsorption process could be divided into three regimes (Fig. 5): it increased instantly at the initial stages, keeps increasing gradually until the equilibrium is reached and then remains constant. However, it should be noted that when the higher copper concentrations (100 and 150 mg/L) were used, these three regimes were less obvious. Furthermore, for both samples SHI-C and SHI-BTCA, a longer time was needed to reach equilibrium when the initial metal concentration was above 75 mg/L.

Different empirical kinetic models, namely Lagergren (Eq. (5)), Ho and McKay (Eq. (6)), Weber and Morris (Eq. (7)), Elovich (Eq. (8)), and Boyd (Eqs. (9) and (10)) plots have been used to test the kinetic experimental data (Azizian, 2004; Plazinski et al., 2009; Qiu et al., 2009; Largite and Pasquier, 2016; Rodrigues and Silva, 2016; Tan and Hameed, 2017; Tran et al., 2017; Kajjumba et al., 2018; Moussout et al., 2018; Zhang et al., 2019; Obradovic, 2020; Benjelloun et al., 2021). The kinetic parameters are listed in Tables 2 and 3, the results obtained by the Chi-square test are given in Table 4, while the plots are reported in Figs. 6 and 7. To distinguish the validity of two models, e.g., between the pseudo-first order and pseudo-second order kinetic equations (Table 2), the best curve-to-data fitting model has been first selected by the highest value of R^2.

3.6. Application of the kinetic models

The pseudo-first-order plot of $\log(q_e\text{-}q_t)$ versus t obtained from our experimental data is given in Fig. 6. The results showed that, although some R^2 values were superior to 0.98, the calculated $q_{e,cal}$ values were not equal to experimental $q_{e,exp}$ values (especially for the higher concentrations), suggesting the insufficiency of the Lagergren model to fit the data for the whole range of initial concentrations for the three selected materials. According to Lagergren's hypothesis, the interpretation of our data indicated that (i) the copper uptake on the material was not governed by a first-order equation; (ii) the pollutant did not adsorb onto adsorbent occupying one localized adsorption site and its concentration was not constant; (iii) the energy of adsorption was dependent on surface coverage; and (iv) adsorption capacity was not proportional to the distance to equilibrium. Finally, the rate-controlling mechanism did not depend on the operating parameters studied and surface coverage (Largitte and Pasquier, 2016; Rodrigues and Silva, 2016; Moussout et al., 2018; Benjelloun et al., 2021).

The equilibrium adsorption capacity $q_{e,exp}$ and equilibrium rate constants of pseudo-second order adsorption (k_2), computed from Eq. (5) and depicted in Fig. 6, along with calculated correlation coefficients are listed in Table 2. The pseudo-second-order or Ho and McKay model is another common and popular model due to its simple mathematical form, which can be applied to fit the experimental data and evaluate the adsorption kinetics. This model, inspired by Blanchard's model (Blanchard et al., 1984), assumes that the uptake is second order concerning the available sites (Ho

Table 2 Pseudo-first order and pseudo-second order kinetic parameters for the adsorption of copper ions onto hemp shives (C_0: initial metal concentration; $q_{e,exp}$ and $q_{e,cal}$: experimental and calculated amount of metal adsorbed at equilibrium, respectively; k_1 and k_2: pseudo-first and pseudo-second order rate constant, respectively; R^2: linear regression coefficient of determination; χ^2: Chi-square test).

Shives	C_0 (mg/L)	Pseudo-first order				Pseudo-second order			
		$q_{e,exp}$ (mg/g)	$q_{e,cal}$ (mg/g)	k_1 (1/min)	R^2	$q_{e,exp}$ (mg/g)	$q_{e,cal}$ (mg/g)	k_2 (g/mg min)	R^2
SHI-W	1	0.05	0.04	0.0290	0.9835	0.05	0.06	1.1100	0.9600
	5	0.30	0.25	0.0292	0.9816	0.30	0.33	0.1960	0.9510
	10	0.60	0.50	0.0293	0.9818	0.60	0.65	0.0979	0.9511
	25	1.48	1.27	0.0302	0.9826	1.48	1.62	0.0397	0.9519
	50	2.08	1.41	0.0251	0.9552	2.08	2.29	0.0278	0.9904
	75	2.83	2.00	0.0285	0.9723	2.83	3.16	0.0203	0.9919
	100	3.32	2.14	0.0206	0.9212	3.32	3.59	0.0171	0.9817
	150	4.06	2.87	0.0285	0.9723	4.06	4.52	0.0142	0.9919
SHI-C	1	0.10	0.03	0.0469	0.8785	0.10	0.11	2.9600	0.9987
	5	0.54	0.12	0.0418	0.7537	0.54	0.55	1.0600	0.9977
	10	1.12	0.68	0.0265	0.9151	1.12	1.17	0.0836	0.9931
	25	2.46	1.03	0.0401	0.8738	2.46	2.53	0.0924	0.9995
	50	5.50	2.55	0.0443	0.8797	5.50	5.72	0.0367	0.9992
	75	6.90	3.84	0.0349	0.9692	6.90	7.16	0.0211	0.9978
	100	8.53	4.88	0.0288	0.9756	8.53	8.87	0.0139	0.9955
	150	9.66	8.13	0.0279	0.9854	9.66	10.42	0.0062	0.9572
SHI-BTCA	1	0.09	0.03	0.0469	0.8685	0.09	0.09	3.2600	0.9985
	5	0.50	0.10	0.0410	0.7263	0.50	0.49	0.9650	0.9996
	10	1.01	0.61	0.0260	0.9056	1.01	1.06	0.0923	0.9924
	25	2.27	0.94	0.0406	0.8519	2.27	2.30	0.1010	0.9996
	50	5.71	2.69	0.0438	0.8904	5.71	5.94	0.0355	0.9994
	75	7.12	3.53	0.0301	0.9232	7.12	7.35	0.0213	0.9982
	100	8.87	5.13	0.0291	0.9683	8.87	9.24	0.0131	0.9957
	150	10.04	8.43	0.0281	0.9835	10.04	10.86	0.0060	0.9541

Table 3 Elovich, Boyd and Weber-Morris kinetic parameters for the adsorption of copper ions onto hemp shives (C_0: initial metal concentration; α and β: Elovich rate constants; *S*: Boyd rate constant; *C*: parameter proportional to the extent of the boundary layer thickness; k_i: intraparticle diffusion rate constant; R^2: linear regression coefficient of determination).

Shives	C_0 (mg/L)	Elovich			Boyd		Weber Morris		
		α (g/mg min)	β (g/mg)	R^2	S^2 (L/min)	R^2	C (mg/g)	K_i (mg/g $min^{1/2}$)	R^2
SHI-W	1	0.009	77.46	0.9864	0.0290	0.9817	0.0177	0.0040	0.9513
	5	0.05	15.22	0.9765	0.0292	0.9795	0.0200	0.0884	0.9637
	10	0.09	7.60	0.9765	0.0293	0.9818	0.1770	0.0401	0.9637
	25	0.23	3.05	0.9766	0.0302	0.9826	0.4480	0.9930	0.9637
	50	0.52	2.46	0.9990	0.0251	0.9552	0.8444	0.1150	0.9668
	75	0.71	1.77	0.9990	0.0285	0.9723	1.2000	0.1550	0.9668
	100	0.88	1.62	0.9848	0.0206	0.9212	1.1600	0.1950	0.9473
	150	1.02	1.24	0.9990	0.0285	0.9692	1.7100	0.2220	0.9668
SHI-C	1	0.12	60.42	0.8084	0.0469	0.8651	0.0879	0.0014	0.8686
	5	1.21	12.27	0.7935	0.0418	0.72635	0.4990	0.0052	0.8686
	10	0.43	4.96	0.9831	0.0265	0.9056	0.5430	0.0530	0.9649
	25	2.84	2.54	0.9432	0.0401	0.8598	1.8000	0.0663	0.9393
	50	4.91	1.08	0.9572	0.0443	0.8797	4.1200	0.1140	0.9802
	75	6.19	0.92	0.9931	0.0349	0.9692	4.2800	0.2520	0.9641
	100	6.11	0.74	0.9965	0.0288	0.9729	4.5800	0.3740	0.9445
	150	1.48	0.47	0.9833	0.0279	0.9837	2.8300	0.6450	0.9969
SHI-BTCA	1	0.11	66.67	0.8084	0.0469	0.8651	0.0769	0.0013	0.7217
	5	1.31	13.94	0.7663	0.0410	0.7263	0.4380	0.0053	0.5804
	10	0.39	5.48	0.9831	0.0265	0.9056	0.4920	0.0481	0.9721
	25	2.32	2.74	0.9424	0.0410	0.8519	1.6700	0.0654	0.7632
	50	5.30	1.05	0.9563	0.0438	0.8904	4.2300	0.1510	0.7494
	75	6.01	0.88	0.9839	0.0301	0.9232	4.5800	0.2410	0.0232
	100	5.65	0.69	0.9914	0.0291	0.9683	4.8200	0.3840	0.9807
	150	1.54	0.45	0.9830	0.0281	0.9835	2.9800	0.6690	0.9531

and McKay, 1998a,b). The numerous works on the adsorption of pollutants onto adsorbents indicated that most kinetic data could be modeled well by this model, suggesting that the rate of adsorption of pollutants is proportional to the available sites on the adsorbent (Renault et al., 2008; Plazinski et al., 2009; Mokkapati et al., 2016; Lopičić et al., 2017; Kajjumba et al., 2018; Moussout et al., 2018; Benjelloun et al., 2021; Bullen et al., 2021). For the range of concentration used in our study, the kinetics of copper adsorption onto shives followed the Ho and McKay model for SHI-W and SHI-C samples (Fig. 6). The calculated $q_{e,cal}$ values agreed with experimental $q_{e,exp}$ values and the R^2 values were higher than 0.99. It was also noted that increasing the metal concentration, the k_2 values decreased, suggesting that adsorption was faster at higher concentrations. A similar observation has been reported before (Azizian, 2004; Crini et al., 2021; Tan and Hameed, 2017). The Ho and Mc Kay also gave a good fit of the experimental data for the SHI-BTCA sample even if the $q_{e,cal}$ values were less similar to those of $q_{e,exp}$ (Table 2).

Considering that pseudo-first and pseudo-second order models cannot clearly identify the adsorption mechanisms (Tran et al., 2017; Benjelloun et al., 2021; Bullen et al., 2021), the intraparticle diffusion model (Weber and Morris, 1963) and the Elovich equation (Elovich and Larinov, 1962; Chien and Clayton, 1980) were further tested in this study.

The intraparticle diffusion model is inspired on the Crank's concept (Crank, 1956) who previously reported that, during the transfer (adsorption) of a pollutant from a solution over a porous adsorbent, three possible cases exist: (1) particle diffusion governance of rate when transport > internal transport; (2) film diffusion governance of rate when external transport < internal transport; and (3) when external transport ≈ internal transport (this case may be excluded since the bulk transport is considered negligible due to their rapid character during the adsorption process) (Walter, 1984). According to the representation proposed in the Weber and Morris model, when an adsorption process is characterized by good mixing, intraparticle diffusion is the rate-controlling step if the plot gives a linear function through the origin, otherwise, film diffusion controls the process (this is the case with poor mixing and low concentration). The variation of q_t versus $t^{1/2}$ is given in Fig. 7. Values of k_i and correlation coefficients are listed in Table 3, from which it can be seen that the kinetics of copper adsorption on the SHI-W and SHI-C samples followed this model with R^2 values higher than 0.95, indicating that intraparticle diffusion was involved in the adsorption process. For these samples, it seems that physisorption (diffusion) played the main role in the adsorption mechanism. However, for the SHI-BTCA, the R^2 values did not support the fact that the metal-adsorption data closely follow this model, suggesting that, in this case, the diffusion mechanism is not the main interaction, and the process was mainly controlled by chemisorption. Nevertheless, for the three selected materials and the entire concentration range studied (1–150 mg/L), it was noted that the adsorption process tends to be followed by two linear regions with non-zero intercepts: the initial curved portion of the plots indicated a boundary layer effect while the second linear portion is due to intraparticle diffusion (Kajjumba et al., 2018). Indeed, the data did not pass through the origin, indicating that intraparticle diffusion was not the

Table 4 Linear R^2 values and non-linear χ^2 values of kinetic models for the adsorption of copper ions onto hemp shives (R^2: linear regression coefficient of determination; χ^2: Chi-square test).

Shives	C_0 (mg/L)	Pseudo-first order	Pseudo-second order	Elovich	Boyd	Weber Morris
		χ^2	χ^2	χ^2	χ^2	χ^2
SHI-W	1	4×10^{-6}	1×10^{-5}	2×10^{-5}	0.0037	4×10^{-6}
	5	0.0001	0.0003	0.0007	0.0035	0.0002
	10	0.0006	0.0011	0.0032	0.0035	0.0007
	25	0.0035	0.0066	0.0202	0.0034	0.0045
	50	0.0058	0.0196	0.0396	0.0072	0.0039
	75	0.6249	0.0323	0.0774	0.0060	0.0068
	100	0.7512	0.0847	0.0997	0.0124	0.0219
	150	1.2779	0.0659	0.1583	0.0060	0.0140
SHI-C	1	2×10^{-5}	1×10^{-5}	0.0003	0.0023	0.0001
	5	0.0003	0.0002	0.0081	0.0015	0.0031
	10	0.0021	0.0065	0.0136	0.0102	0.0020
	25	0.3192	0.0228	0.0963	0.0060	0.0185
	50	1.7490	0.1188	0.4521	0.0046	0.0824
	75	2.3231	0.3235	0.3706	0.0101	0.0192
	100	3.5819	0.5907	0.4085	0.0121	0.0105
	150	8.8247	0.1582	0.6383	0.0021	0.0747
SHI-BTCA	1	1×10^{-5}	2×10^{-5}	0.0001	0.0023	0.0003
	5	0.0003	0.0005	0.0028	0.0468	0.0068
	10	0.0054	0.0017	0.0017	0.0095	0.0112
	25	0.0147	0.2751	0.0162	0.9409	0.0828
	50	0.1166	1.8529	0.0822	15.7898	0.4823
	75	0.2785	2.5685	0.0404	23.6858	0.4500
	100	0.5090	4.1204	0.0246	36.2371	0.5004
	150	0.1536	9.6173	0.0858	36.4554	0.7138

only rate-limiting mechanism and that some other interactions also played an important role. The calculated k_i values for each initial concentration (Table 3) indicated that, when the metal concentration was augmented, the rate constant increased for all the tested samples. The values of C (boundary layer thickness) also increased with copper concentration (higher values, the greater the effect). However, the analysis of the data indicated that deviations from Weber and Morris model mainly occurred at high initial metal concentrations. Similar interpretations on this were reported before (Qiu et al., 2009; Reddy et al., 2012; Largitte and Pasquier, 2016; Mokkapati et al., 2016; Kajjumba et al., 2018; Obradovic, 2020).

The Elovich model, inspired by Zeldowitsch's model (Zeldowitsch, 1934) and developed for gaseous systems, helps to predict the mass and surface diffusion, activation and deactivation energy of a given system, determining the nature of adsorption on the heterogeneous surface of the adsorbent, whether chemisorption or not (Kajjumba et al., 2018). This model is expressed by Eq. (8) where α and β are the initial rate and desorption constant, respectively, during any experiment (Elovich and Larinov, 1962). Fig. 6 shows that, for the three selected samples, the metal adsorption also fitted the Elovich equation, suggesting a chemisorption mechanism such as surface complexation formation and that shives surfaces are energetically heterogeneous. Table 3 lists the kinetic constants. The values of initial adsorption rate (α) and desorption constant (β) varied in function of the copper concentration. In particular, when the concentration increased, the β constant decreased for both SHI-C and SHI-BTCA samples, suggesting a decrease in the availability of adsorption sites for copper adsorption (Renault et al., 2008; Vaghetti et al., 2009; Lopičić et al., 2017; Tan and Hameed, 2017). The analysis of the data clearly indicated that the Elovich model gave the best fit for the experimental data obtained for the SHI-BTCA sample, confirming the involvement of the carboxylate groups in the adsorption mechanism. Nevertheless, the data were also well simulated by the Elovich model for SHI-W and SHI-C samples, indicating the mechanism was complicated with the presence of both chemisorption (complexation) and physisorption (diffusion).

By applying the Lagergren, Ho and McKay, and Elovich models, it is assumed that the overall adsorption process rate is governed by the rate of binding, whereas when applying the Weber and Morris model, the rate of mass transport is expected to govern the overall process rate (Obradovic, 2020). The Boyd model is also an adsorption diffusion model used to predict the mechanistic steps involved in an adsorption process, i.e., whether the rate of removal of the metal takes place *via* film diffusion or particle diffusion mechanism (Boyd et al., 1947a,1947b). If the plot is a straight line passing through the origin, then adsorption is governed by a particle-diffusion mechanism, otherwise governed by film diffusion (Okewale et al., 2013; Benjelloun et al., 2021). An analysis of the literature shows that, in numerous works, film diffusion is the limiting step during the initial stages of the adsorption process followed by intraparticle diffusion when pollutant species reach the material surface (Kajjumba et al., 2018). However, it is difficult to estimate appropriate values of *Bt* for the entire time scale, so the data should be carefully interpreted. The good correlation obtained between the experimental data and predicted curves proved the validity of the Boyd

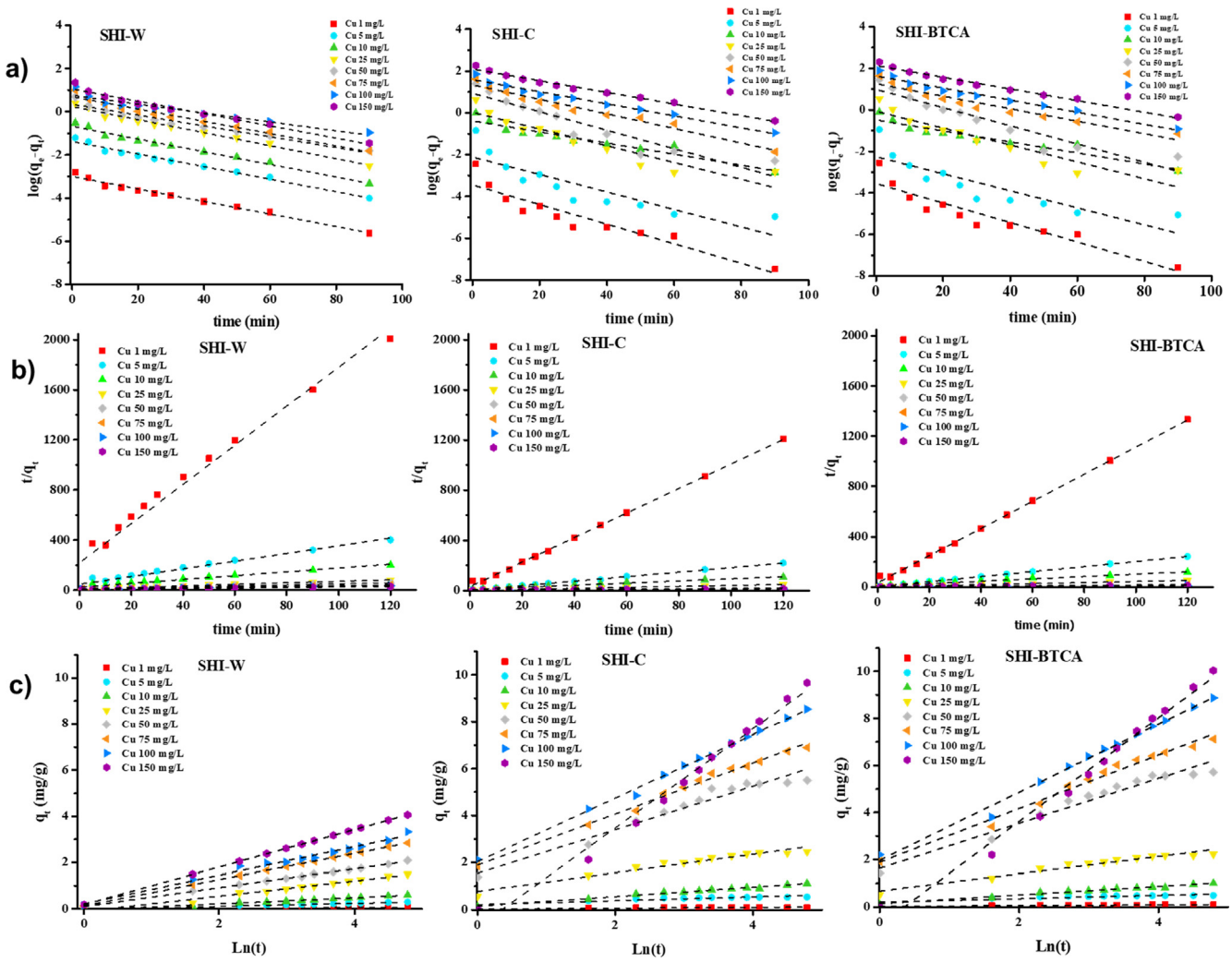

Fig. 6 Lagergren (a), Ho and McKay (b), and Elovich (c) plots for copper adsorption onto SHI-W, SHI-C and SHI-BTCA.

model only for the SHI-W sample, with R^2 values higher than 0.95 (Table 4). For the two other samples, the Boyd model did not adequately fit the data. In addition, as shown in Fig. 7, the plots for the three materials did not pass through the origin, revealing that the film diffusion controls the process for the copper adsorption onto three samples.

3.7. Goodness of fit of the plots

The analysis of kinetic modeling indicated that these data should be plotted with the experimental data in the non-linear form of the model equation used and predicted throughout the adsorption period. Selecting the appropriate model and analyzing the results of the modeling deserves a careful interpretation, whereas using only the quality of the fittings by determining the coefficient correlation values is not sufficient (Tran et al., 2017). Due to the inherent bias resulting from the linearization of models, a non-linear chi-square test (χ^2) was also used to confirm the best-fit kinetic equation to the experimental data. Table 4 presents the results of fitting experimental data with the five kinetic models using χ^2 values. The comparison of error analysis indicated that the order of deviation was:

- Lagergren > Elovich > Ho and McKay > Weber and Morris > Boyd for SHI-W and SHI-C samples;
- Boyd > Ho and McKay > Weber and Morris > Lagergren > Elovich for SHI-BTCA sample.

For SHI-W and SHI-C samples, the Boyd model was the best at describing the adsorption kinetics of copper, suggesting the predominance of the physisorption (diffusion) in the adsorption process. The order obtained for SHI-BTCA indicated that the Elovich model gave the best fitting for the experimental data since the lowest χ^2 values were obtained with R^2 values greater than 0.95 in comparison to other models. The applicability for the Elovich model described chemisorption (complexation) on highly heterogeneous adsorbents (Zhang et al., 2019). However, the adsorption mechanism is much more complex as it Involves several interactions such as complexation, ion-exchange and microprecipitation. To confirm this, a preliminary study by coupling energy-disperse X-ray (EDX) spectroscopy and X-ray computed nanotomography (nano-CT) was carried out.

Fig. 8 reports EDX spectra and nano-CT images of hemp shives samples before and after copper adsorption. In the EDX spectra obtained for SHI-BTCA, the replacement of

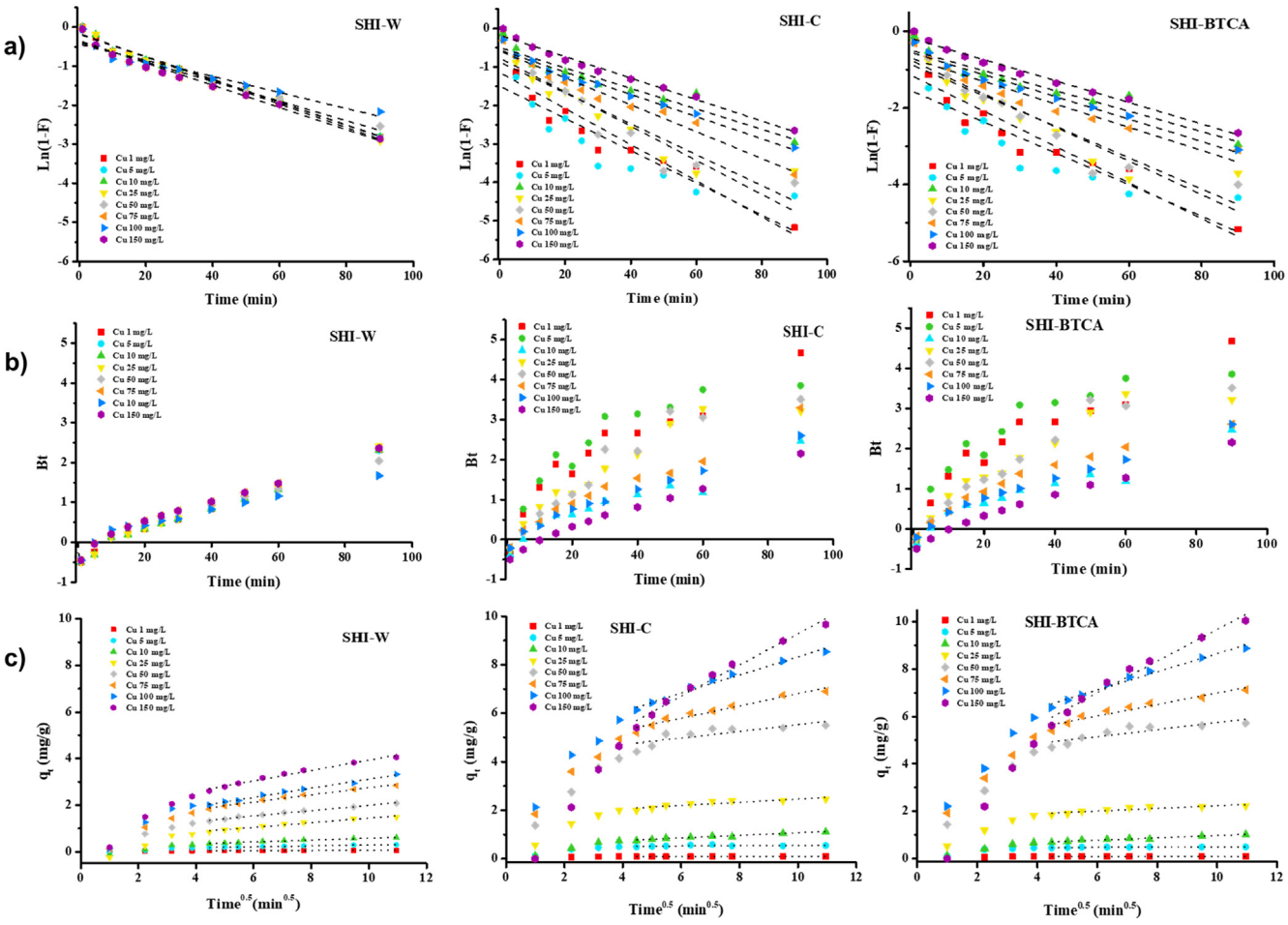

Fig. 7 Boyd (a and b) and Weber and Morris (c) plots for copper adsorption onto SHI-W, SHI-C and SHI-BTCA.

the sodium at the surface of the fibres by copper indicated the presence of an ion-exchange mechanism, in agreement with the increase of the values of sodium concentrations after adsorption. Copper is also observed in all three EDX spectra after adsorption. The nano-CT images obtained before copper adsorption illustrate the modification of the cell wall obtained after treatment with BTCA compared to the SHI-W and SHI-C. Indeed, after BTCA grafting, it is observed a collapse of the structure with a distortion of the vessels, a degradation of the woody rays and a fully disorganization of the tissues. This is in agreement with the important decrease of porosity value and the change in the chemical composition (Table 1). Nevertheless, for SHI-C sample, the fiber walls are also affected by the treatment due to the removal of a part of the hemicelluloses leading to a partial deconstruction of the cell wall of the woody fibers (Fig. 8). After copper adsorption, the metal distribution showed in red in the 3D images is totally different for the samples. For SHI-C and SHI-W, the copper is diffused on all the free surfaces (confirming the physisorption) while for SHI-BTCA, the copper is mainly adsorbed on the external surface of the shives, suggesting the involvement of the carboxylate groups grafted in the surface of the shives. All these data demonstrated that the adsorption mechanism for the three materials is different.

4. Conclusion

In this study, a series of hemp shives with different surface properties were used as adsorbents for copper removal in batch experiments. The adsorbents were a raw sample (SHI-R), a washed sample with water (SHI-W), three samples activated by chemical reagents such as KOH (SHI-OH), Na_2CO_3 (SHI-C) and H_3PO_4 (SHI-H), and a material prepared from a grafting of carboxylic groups (SHI-BTCA). Adsorption data indicated that, for the same experimental conditions, the order in terms of performance to recover copper was: SHI-C ~ SHI-BTCA > SHI-OH ≫ SHI-W > SHI-R ≫ SHI-H. In the case of studied parameters (metal concentration, adsorbent dose and contact time), SHI-C and SHI-BTCA samples had the highest levels of copper removal with an equilibrium time of 60 min. A detailed kinetic study of the experimental data using five common models showed that the orders obtained were Lagergren < Elovich < Ho and McKay < Weber and Morris < Boyd *vs.* Boyd < Ho and McKay < Weber and Morris < Lagergren < Elovich for SHI-C and SHI-BTCA, respectively. The analysis of the results indicated that chemisorption played the main role in the copper adsorption onto the SHI-BTCA while physisorption (diffusion) was the main interaction with SHI-C. However, the adsorption mechanisms are much more complex as they involve several interactions at the same time. To clearly demonstrate these mechanisms, we will characterize these interactions using spectroscopic tools such as Raman, X-ray photoelectron spectroscopy, and X-ray absorption near-edge structure spectroscopy.

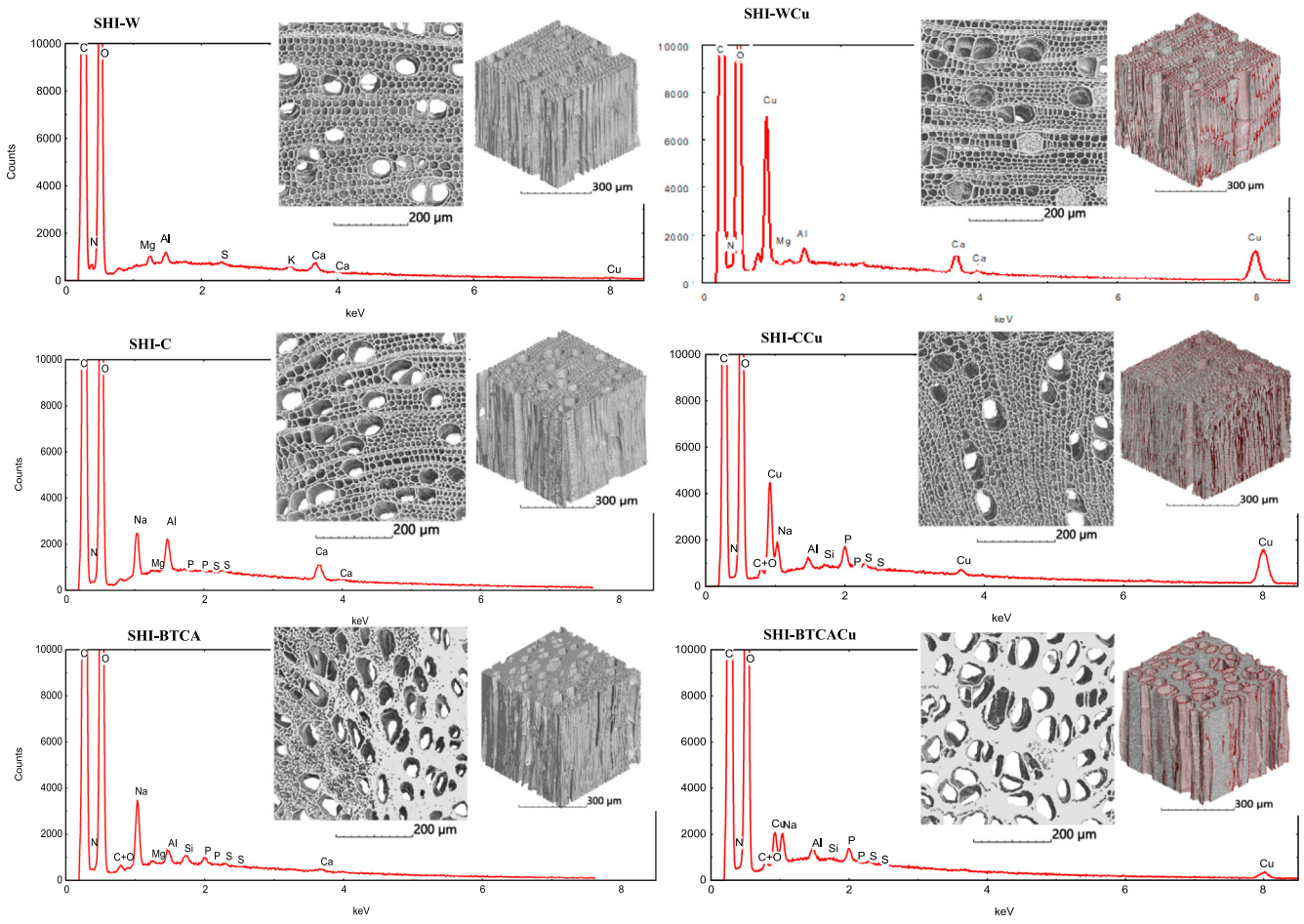

Fig. 8 Elemental analysis using energy-disperse X-ray spectra and X-ray computed nanotomography (images in 3D) of hemp shives samples before (left) and after (right) adsorption of copper (the high intensity voxels corresponding to Cu elements are in red colour in the density-based segmentation of the X-ray images).

Declaration of Competing Interest

The authors declare that they have no known competing financial interests that could have appeared to influence the work reported in this paper.

Acknowledgement

N. Morin-Crini and G. Crini thank Eurochanvre (Arc-les-Gray, France) for the gift of the materials, *Région Bourgogne Franche-Comté* (France) and FEDER (*Fonds Européen de Développement Régional*) for financial support, and the PEA^{2}t Platform (Chrono-environnement, *Université Bourgogne Franche-Comté,* France) which manages and maintains the analytical equipment used in this study. X. Gabrion, V. Placet and M. Raschetti are grateful to MIFHySTO technological platform (FEMTO-ST, France) for the use of EDX and computed tomography equipment. The doctoral student Chiara Mongioví also thanks the *Région Bourgogne Franche-Comté* (France) for awarding her a research grant. A.R.L. Ribeiro would like to thank FCT funding under the DL57/2016 Transitory Norm Programme and the scientific collaboration under project Base-UIDB/50020/2020 and Programmatic-UIDP/50020/2020 funding of LSRE-LCM, funded by national funds through FCT/MCTES (PIDDAC).

References

Al-Saydeh, S.A., El-Naas, M.H., Zaidi, S.J., 2017. Copper removal from industrial wastewater: a comprehensive review. J. Ind. Eng. Chem. 56, 35–44.

Azizian, S., 2004. Kinetic models of sorption: a theoretical analysis. J. Colloid. Int. Sci. 276, 47–52.

Barakat, M.A., Kumar, R., 2015. Modified and new adsorbents for removal of heavy metals from wastewater. In: Sharma, S.K. (Ed.), Heavy Metals in Water: Presence, Removal and Safety. The Royal Society of Chemistry, chapter10, pp. 193–212.

Bashir, M., Tyagi, S., Annachhatre, A.P., 2020. Adsorption copper from aqueous solution onto agricultural adsorbent: Kinetics and isotherm studies. Mater. Today: Proc. 28, 1833–1840.

Benjelloun, M., Miyah, Y., Evrendilek, G.A., Zerrouq, F., Lairini, S., 2021. Recent advances in adsorption kinetic models: their application to dye types. Arabian. J. Chem. 14, 103031.

Blanchard, G., Maunaye, M., Martin, G., 1984. Removal of heavy metals from waters by means of natural zeolites. Water Res. 18, 1501–1507.

Boyd, G.E., Schubert, J., Adamson, A.W., 1947a. The exchange adsorption of ions from aqueous solutions by organic zeolites. I. Ion-exchange equilibria. J. Am. Chem. Soc. 69, 28186–32829.

Boyd, G.E., Adamson, A.W., Myers Jr., L.S., 1947b. The exchange adsorption of ions from aqueous solutions by organic zeolites. II. Kinetics. J. Am. Chem. Soc. 69, 2836–2848.

Bullen, J.C., Saleesongsom, S., Gallagher, K., Weiss, D.J., 2021. A revised pseudo-second-order kinetic model for adsorption, sensitive to changes in adsorbate and adsorbent concentrations. Langmuir 37, 3189–3201.

Crank, J., 1956. The mathematics of diffusion. Oxford Science Publications. Oxford University Press, London.

Chien, S.H., Clayton, W.R., 1980. Application of Elovich equation to the kinetics of phosphate release and sorption in soils. Soil Sci. Soc. Am. J. 44, 265–268.

Crini, G., Lichtfouse, E., 2020. Hemp Production and Applications. Sustainable Agriculture Reviews 42. Springer Nature Switzerland, Cham.

Crini, G., Lichtfouse, E., Chanet, G., Morin-Crini, N., 2020. Applications of hemp in textiles, paper industry, insulation and building materials, horticulture, animal nutrition, food and beverages, nutraceuticals, cosmetics and hygiene, medicine, agrochemistry, energy production and environment. Environ. Chem. Lett. 18, 1451–1476.

Crini, G., Bradu, C., Cosentino, C., Staelens, J.N., Martel, B., Fourmentin, M., Loiacono, S., Chanet, G., Torri, G., Morin-Crini, N., 2021. Simultaneous removal of inorganic and organic pollutants from polycontaminated wastewaters on modified hemp-based felts. Rev. Chim. 72, 25–43.

Ducoroy, L., Martel, B., Bacquet, M., Morcellet, M., 2007. Cation exchange finishing of nonwoven polyester with polycarboxylic acids and cyclodextrins. J. Appl. Polym. Sci. 03, 3730–3738.

Dunford, N.T., 2015. Hemp and flaxseed oil: properties and applications for use in food. In: Talbot, G. (Ed.), Specialty Oils and Fats in Food and Nutrition: Properties, Processing and Applications. Elsevier, pp 39–63.

Elgarahy, A.M., Elwakeel, K.Z., Mohammad, S.H., 2021. A critical review of biosorption od dyes, heavy metals and metalloids from wastewater as an efficient and green process. Clean. Eng. Technol. 4, 100209.

Elovich, S.Y., Larinov, O.G., 1962. Theory of adsorption from solutions of non electrolytes on solid (I) equation adsorption from solutions and the analysis of its simplest form, (II) verification of the equation of adsorption isotherm from solutions. Izvest. Akad. Nauk SSSR, Otdelenie Khimicheskikh Nauk 2, 209–216.

Gupta, V.K., Nayak, A., Agarwal, S., 2015. Bioadsorbents for remediation of heavy metals: current status and their future prospects. Environ. Eng. Res 20, 1–18.

Ho, Y.S., McKay, G., 1998a. Kinetic models for the sorption of dye from aqueous solution by wood. TransI. ChemE 76, 183–191.

Ho, Y.S., McKay, G., 1998b. A comparison of chemisorption kinetic models applied to pollutant removal on various sorbents. TransI. ChemE 76, 332–340.

Ingrao, C., Lo Giudice, A., Bacenetti, J., Tricase, C., Dotelli, G., Fiala, M., Siracusa, V., Mbohwa, C., 2015. Energy and environmental assessment of industrial hemp for building applications: a review. Renew. Sust. Energ. Rev. 51, 29–42.

Ivanovska, A., Pavun, L., Dojčinović, B., Kostić, M., 2021. Kinetic and isotherm studies for nickel ions' biosorption by jute fabrics. J. Serb. Chem. 86, 885–897.

Jamoussi, B., Chakroun, R., Jablaoui, C., Rhazi, L., 2020. Efficiency of *Acacia gummifera* powder as biosorbent for simultaneous decontamination of water polluted with metals. Arab. J. Chem. 13, 7459–7481.

Jiang, Y., Ansell, M.P., Jia, X., Hussain, A., Lawrence, M., 2017. Physical characterization of hemp shiv: cell wall structure and porosity. Acad. J. Civil Eng. 35, 22–28.

Kajjumba, G.W., Emik, S., Öngen, A., Özcan, H.K., Aydın, S., 2018. Modelling of adsorption kinetic processes – errors, theory and application. In: Serpil Edebali S. (Ed.), Advanced Sorption Process Applications, Chapter 10, pp. 1–19.

Kostić, M., Vukčević, M., Pejić, B., Kalijadis, A., 2014. Hemp fibers: old fibers – new applications. In: Ibrahim, Md., Mondal, M. (Eds.), Textiles: History, Properties and Performance and Applications. Nova Science Publishers, New York, Inc. pp 399–446.

Lagergren, S., 1898. Zur theorie der sogenannten adsorption gelster stoffe. Kung. Svensk. Vetenskapsakad. Hand. Band. 24, 1–39.

Largite, L., Pasquier, R., 2016. A review of the kinetics adsorption models and their application to the adsorption of lead by an activated carbon. Chem. Eng. Res. Design 109, 495–504.

Lessa, E.F., Medina, A.L., Ribeiro, A.S., Fajardo, A.R., 2020. Removal of multi-metals from water using reusable pectin/cellulose microfibers composite beads. Arab. J. Chem. 13, 709–720.

Loiacono, S., Crini, G., Martel, B., Chanet, G., Cosentino, C., Raschetti, M., Placet, V., Torri, G., Morin-Crini, N., 2017. Simultaneous removal of Cd Co, Cu, Mn, Ni, and Zn from synthetic solutions on a hemp-based felt. II. Chemical modification. J. Appl. Polym. Sci. 134, 45138.

Loiacono, S., Crini, G., Chanet, G., Raschetti, M., Placet, V., Morin-Crini, N., 2018a. Metals in aqueous solutions and real effluents: biosorption behavior onto a hemp-based felt. J. Chem. Technol. Biotechnol. 93, 2592–2601.

Loiacono, S., Morin-Crini, N., Martel, B., Chanet, G., Bradu, C., Torri, G., Crini, G., 2018b. Complexation du zinc, du cuivre et du manganèse par du chanvre: efficacité chimique et impact écotoxicologique (in French). Environ. Risques Santé 17, 240–252.

Lopičić, Z.R., Stojanović, M.D., Kaluderović Radoičić, T.S., Milojković, J.V., Petrović, M.S., Mihajlović, M.L., Kijevčanin, M.L.J., 2017. Optimization of the process of Cu(II) sorption by mechanically treated *Prunus persica* L. – contribution to sustainability in food processing industry. J. Clean. Prod. 156, 95–105.

Lopičić, Z.R., Stojanović, M.D., Marković, S.B., Milojković, J.V., Mihajlović, M.L., Kaluderović Radoičić, T.S., Kijevčanin, M.L.J., 2019. Effects of different mechanical treatments on structural changes of lignocellulosic waste biomass and subsequent Cu(II) removal kinetics. Arab. J. Chem. 12, 4091–4103.

Mokkapati, R.P., Mokkapati, J., Ratnakaram, V.N., 2016. Kinetic, isotherm and thermodynamics investigation on adsorption of divalent copper using agro-waste biomaterials, *Musa acuminata*, *Casuarina equisetifolia* L. and *Sorghum bicolor*. Polish J. Chem. Technol. 18, 2, 68–77.

Mongioví, C., Lacalamita, D., Morin-Crini, N., Gabrion, X., Ivanovska, A., Sala, F., Placet, V., Rizzi, V., Gubitosa, J., Mesto, E., Ribeiro, A.R.L., Fini, P., De Vietro, N., Schingaro, E., Kostić, M., Cosentino, C., Cosma, P., Bradu, C., Chanet, G., Crini, G., 2021. Use of chènevotte, a valuable co-product of industrial hemp fiber, as adsorbent for pollutant removal. Part I: Chemical, microscopic, spectroscopic and thermogravimetric characterization of raw and modified samples. Molecules 26, 4574.

Moussout, H., Ahlafi, H., Aazza, M., Mahat, H., 2018. Critical of linear and nonlinear equations for pseudo-first order and pseudo-second order kinetic models. Karbala Int. J. Modern Sci. 4, 244–254.

Morin-Crini, N., Loiacono, S., Placet, V., Torri, G., Bradu, C., Kostić, M., Cosentino, C., Chanet, G., Martel, B., Lichtfouse, E., Crini, G., 2019. Hemp-based adsorbents for sequestration of metals. Environ. Chem. Lett. 17, 393–408.

Obradovic, B., 2020. Guidelines for general adsorption kinetics modeling. Hem. Ind. 74, 65–70.

Okewale, A.O., Babayemi, K.A., Olalekan, A.P., 2013. Adsorption isotherms and kinetic models of starchy adsorbents on uptake of water from ethanol-water systems. Int. J. Appl. Sci. Technol. 3, 35–42.

Plazinski, W., Rudzinski, W., Plazinska, A., 2009. Theoretical models of sorption kinetics including a surface reaction mechanism: a review. Adv. Colloid Int. Sci. 152, 2–13.

Paliulis, D., 2021. Removal of lead(II) and zinc(II) from aqueous solutions applying fiber hemp (Cannabis sativa L.). Ecol. Chem. Eng. S. 28, 229–239.

Qasem, N.A.A., Mohammed, R.H., Lawal, D.U., 2021. Removal of heavy metal ions from wastewater: a comprehensive and critical review. Clean Water 36, 1–15.

Qiu, H., Lv, L., Pan, B.C., Zhang, Q.J., Zhang, W.M., Zhang, Q.X., 2009. Critical review in adsorption kinetic models. J. Zhejiang Univ. A 10, 716–724.

Rashid, R., Shafiq, I., Akhter, P., Iqbal, M.J., Hussain, M., 2021. A state-of-the-art review on wastewater treatment techniques: The effectiveness of adsorption method. Environ. Sci. Pollut. Res. 28, 9050–9066.

Reddy, D.H.K., Lee, S.M., Seshaiah, K., 2012. Removal of Cd(II) and Cu(II) from aqueous solution by agro biomass: Equilibrium, kinetic and thermodynamic studies. Environ. Eng. Res. 17, 125–132.

Renault, F., Morin-Crini, N., Gimbert, F., Badot, P.M., Crini, G., 2008. Cationized starch-based material as a new ion-exchanger adsorbent for the removal of C.I. Acid Blue 25 from aqueous solutions. Bioresour. Technol. 99, 7573–7586.

Rodrigues, A.E., Silva, C.M., 2016. What's wrong with Lagergren pseudo first order for adsorption kinetics? Chem. Eng. J. 306, 1138–1142.

Rozumová, L., Legátová, B., Prehradná, J., 2018. Potential of the biosorbents from waste for the separation of Cu(II) from aqueous solutions. Key Eng. Mater. 779, 102–109.

Rozumová, L., Legátová, B., 2018. Biosorbent from industrial hemp hurds for copper ions removal. Int. J. Mater. Sci. Eng. 6, 114–125.

Schwaab, M., Steffani, E., Barbosa-Coutinho, E., Severo Junior, J.B., 2017. Critical analysis of adsorption/diffusion modelling as a function of time square root. Chem. Eng. J. 173, 179–186.

Solioz, M., 2018. Copper and Bacteria. Evolution, Homeostasis and Toxicity. Springer International Publishing, p. 88 p..

Tan, K.L., Hameed, B.H., 2017. Insight into the adsorption kinetics models for the removal of contaminants from aqueous solutions. J. Taiwan Institute Chem. Eng. 74, 25–48.

Tofan, L., Păduraru, C., Teodosiu, C., 2020. Hemp fibers for wastewater treatment. In: Crini, G., Lichtfouse, E. (Eds.), Hemp Production and Applications. Sustainable Agriculture Reviews, vol. 42, pp. 295–326.

Torres, E., 2020. Biosorption: A review of the latest advances. Processes 8, 1584.

Tran, H.N., You, S.J., Hosseini-Bandegharaei, A., Chao, H.P., 2017. Mistakes and inconsistencies regarding adsorption of contaminants from aqueous solutions: a critical review. Water Res. 120, 88–116.

Vaghetti, J.C.P., Lima, E.C., Royer, B., da Cunha, B.M., Cardoso, N. F., Brasil, J.L., Dias, S.L.P., 2009. Pecan nutshell as biosorbent to remove Cu(II), Mn(II) and Pb(II) from aqueous solutions. J. Hazard. 162, 270–280.

Wahid, F., Mohammadzai, I.U., Khan, A., Shah, Z., Hassan, W., Ali, N., 2017. Removal of toxic metals with activated carbon prepared from *Salvadora species*. Arab. J. Chem. 10, S2205–S2212.

Walter, W.J., 1984. Evolution of a technology. J. Environ. Eng. 110, 899–917.

Weber, W.J., Morris, J.C., 1963. Kinetics of adsorption of carbon from solution. J. Sanit. Eng. Div. 89, 31–59.

Wong, H.W., Ibrahim, N., Hanif, M.A., Mohamed, Noor N., Yusuf, S.Y., Hasan, M., 2020. Optimization of copper adsorption from synthetic wastewater by oil palm-based adsorbent using central composite design. In: IOP Conf. Series: Earth and Environmental Science, vol. 476, pp. 012104.

Zare, H., Heydarzade, H., Rahimnejad, M., Tardast, A., Seyfi, M., Peyghambarzadeh, S.M., 2015. Dried activated sludge as an appropriate biosorbent for removal of copper (II) ions. Arab. J. Chem. 8, 858–864.

Zeldowitsch, J., 1934. Über den mechanimus der katalytischen oxidation von CO a MnO_2. Acta Physicochem. URSS 1, 364–449.

Zhang, R., Leiviskä, T., Tanskanen, J., Gao, B.Y., Yue, Q.Y., 2019. Utilization of ferric groundwater treatment residuals for inorganic-organic hybrid biosorbent preparation and its use for vanadium removal. Chem. Eng. J. 361, 680–689.